



Precious and structural metals on asteroids

Kevin M. Cannon^{a,b,*}, Matt Gialich^c, Jose Acain^c

^a Department of Geology and Geological Engineering, Colorado School of Mines, Golden, CO, 80401, USA

^b Space Resources Program, Colorado School of Mines, Golden, CO, 80401, USA

^c AstroForge Inc., Huntington Beach, CA, 92649, USA

ARTICLE INFO

Keywords:

Asteroid

ISRU

Metal

Space resources

Meteorite

ABSTRACT

Metals and metallic elements in silicate/oxide form are abundant in asteroid materials and are often touted as a valuable space resource that can be returned to Earth or used in space. However, the data that come along with these claims are decades old, incomplete, and of questionable quality. Here, we draw on newer measurements and statistics from the vast meteorite collection to assess the concentrations of many elements in likely asteroid materials compared to terrestrial ore deposits. A cursory comparison of 83 elements identifies a promising group that are examined in more detail: the platinum group metals (PGMs) Rh, Ru, Pd, Os, Ir, Pt, and the base metals Fe, Mg, Al, and Si. PGMs are found to deviate from chondritic ratios with respect to Ir at higher Ir values, such that maximum PGM contents in asteroids likely do not reach as high as previously thought. However, there may be other strategies to form a PGM-rich concentrate, for example separating out refractory metal nuggets from more primitive undifferentiated asteroids. In addition to precious metals, the base metals Fe, Mg, Al, and Si can be chemically reduced and used to support in-space manufacturing, particularly for large space structures and solar panels. In all cases, the path from raw asteroid material to refined products can be organized using the concept of flowsheets from terrestrial mining, where mineral processing/beneficiation is of first-order importance.

1. Introduction

Natural resources on the Moon, Mars, and asteroids will allow humanity to expand further into space and can also improve conditions on Earth by moving heavy industry off planet (Metzger et al., 2013) or pursuing efforts like space-based solar power. Asteroids are attractive in the longer term because there are abundant and diverse types beyond the orbit of Mars en route to the outer solar system. The total mass of the asteroids is low compared to planets and moons, but only a thin outer shell of those larger bodies can be reached by excavation (Fig. 1). Conversely, asteroids are small enough to be deconstructed with tractable energy inputs, opening a much larger accessible mining volume (AMV), defined here as:

$$AMV = \begin{cases} \frac{4}{3}\pi r^3 & \text{if } r \leq 5E5 \text{ m} \\ \frac{4}{3}\pi(r^3 - (r - 1200)^3) & \text{otherwise} \end{cases}$$

This accessible volume for the main belt exceeds the combined values for Mars, Mercury, and the Moon (even when Ceres and Vesta are

excluded). The near-Earth asteroids could provide precious metals, and water for cislunar propellant in the near term if they end up trading favorably with lunar material (Colvin et al., 2020; Sowers, 2021). But with $100,000 \times$ lower accessible volume than the main belt they may not be a significant source of bulk materials in the longer term.

Precious metals are cited in popular media as an immensely valuable trove in space, but the reality is more nuanced. Asteroid resources include volatile species (H, C, O, etc.), silicate minerals appropriate for further processing including reducing them to produce metals, and already-reduced metals (overwhelmingly Fe and Ni). Most of these materials will not be economic to return to Earth in the near term and may never be. However, platinum group metals (PGMs) which include Rh, Ru, Pd, Os, Ir, and Pt have been a motivating factor for asteroid mining and are purported to reach high enough concentrations in M-type asteroids to consider sourcing them from space (Kargel, 1994; Lewis, 1996; Elvis, 2014). Other similarly enriched elements include Re and Au. M-type asteroids are the class introduced by Chapman et al. (1973) based on telescopic spectra and are commonly equated as “metallic”. The M-type from the taxonomy in Tholen (1984) was subsumed into the grab-bag “X-Complex” in the Bus and Bus-DeMeo taxonomies (DeMeo et al., 2009) but has since been resurrected in a more recent classification from

* Corresponding author. Geology and Geological Engineering, 1301 19th St., Golden, CO, 80401-1705, USA.

E-mail address: cannon@mines.edu (K.M. Cannon).

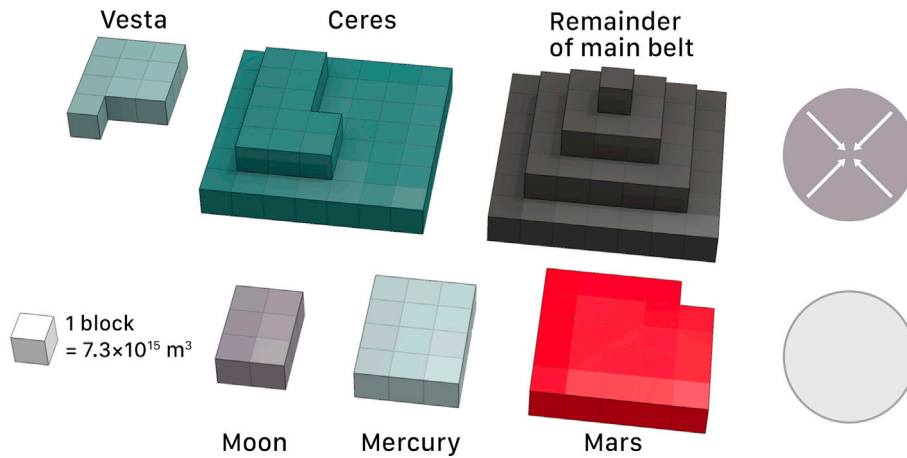


Fig. 1. To-scale accessible mining volume of terrestrial bodies, calculated as the total volume for the asteroids (main belt mass of 2.39×10^{23} kg, mean bulk density of 2000 kg/m^3), and as the volume for an outer shell 1.2 km in thickness for the Moon, Mercury, and Mars, equivalent to the deepest open pit mine on Earth. Note the combined volume of the near-Earth asteroids ($\sim 5 \times 10^{12} \text{ m}^3$) is too small to be visible at this scale.

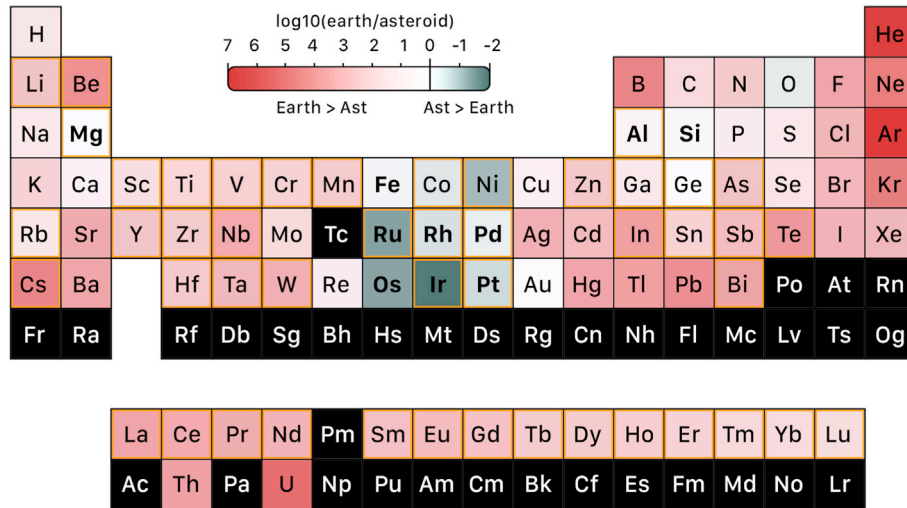


Fig. 2. Ratios of the maximum concentrations of elements found in likely asteroid material (Koblitz, 2003 and references therein) compared to high-grade or typical ores on Earth. Yellow borders indicate critical minerals according to the U.S. Geological Survey. Elements in bold are investigated in more detail in this study.

Mahlke et al. (2022). PGMs are some of the most expensive materials known, for example Rh has a market price $> \$500,000 \text{ USD/kg}$ and only about 20–30 tons are mined per year (Gunn, 2013). There could be an emerging case to return these metals given the down mass capability of SpaceX's Starship (~ 50 tons), but data on asteroid metal concentrations and economic potential are lacking. Most papers simply cite the 90th percentile concentrations listed by Kargel (1994) based on iron meteorites and LL chondrites. Upon further investing the Kargel (1994) data they are found to be incomplete. Kargel used measurements of *Ir* only, then assumed all other PGMs and Au vary linearly with *Ir* according to chondritic ratios. As we show below, this assumption does not hold. Additionally, our concept of M-types as monolithic blocks of pure metal has been significantly challenged since that time (Shepard et al., 2008, 2010, 2015; Viikinkoski et al., 2018); even the archetypal M-type (16) Psyche may not be a pure metal body (Elkins-Tanton et al., 2022), such that other asteroid classes which host PGMs in different mineral forms should be considered.

Metals used for in-space applications (structural components, photovoltaic cells) will eventually have more value than precious metals returned to Earth, but they are much harder to price accurately. The light metals Al and Mg have diverse use cases and are appropriate for large structures like trusses or beams. Fe will be useful in cases where the

properties of steel are more desirable than Al or Mg. And nothing will be done in space without power, which will predominantly come from solar photovoltaics made to a large extent from Si. Other metals like Ni, Co, Cu and Rare Earth Elements (REEs) have niche applications but are less likely to be produced in-space en masse as bulk materials in the near to mid future. The structural/photovoltaic metals have received far less attention as asteroid resources, perhaps because of the appeal of riches from platinum and gold. What are their concentrations on different types of asteroids? Which mineral phases are they found in, and can mineral processing/beneficiation be used to upgrade their concentrations before extracting and refining them?

The goal of this work is to improve our picture of metal contents on asteroids including both precious metals (some of which could be returned to Earth) and structural/photovoltaic metals (for in-space use). Meteorite grades of 83 elements are compared to terrestrial ores, which set the appropriate baseline values rather than bulk Earth crust. The most promising metals for potential return to Earth and in-space use are identified and examined in more detail using up-to-date measurements of meteorites. Finally, asteroid exploration and processing strategies are discussed based on the likely speciation and concentrations of these elements.

Table 1
Sources of PGM data used in this work.

Reference	Iron Meteorite Group(s)	Measurement Technique
Wasson and Richardson (2001)	IVA	INAA ^a
Wasson and Richardson (2001)	IAB	INAA
Petaev and Jacobsen (2004)	IAB, IIAB, IIIAB, IID, IVA, IVB IC	LA-ICP-MS ^b
Campbell and Humayun (2005)	IVB	LA-ICP-MS
Wasson and Huber (2006)	IID	INAA
Wasson et al. (2007)	IIAB	INAA
Walker et al. (2008)	IVB	ID-ICP-MS ^c
McCoy et al. (2011)	IVA	LA-ICP-MS, ID-ICP-MS
Worsham et al. (2016)	IAB	ID-ICP-MS
Wasson (2017)	IIE	INAA
Tornabene (2020)	IC	ID-ICP-MS
Tornabene et al. (2020)	IIC	ID-ICP-MS
Chabot and Zhang (2022)	IIIAB	INAA
Hilton et al. (2022)	IIAB, IIIAB, IID, IIIF	ID-ICP-MS
Zhang et al. (2022a)	IIIF	LA-ICP-MS, INAA
Zhang et al. (2022b)	IVB, IIC, IIIF	INAA

^a Instrumental Neutron Activation Analysis.

^b Laser Ablation Inductively Coupled Plasma Mass Spectrometry.

^c Isotope Dilution Inductively Coupled Mass Spectrometry.

2. Data sources and methods

2.1. Meteorite concentrations

Most meteorites are fragments of asteroids and provide the best guide for elemental abundances on their parent bodies. There are challenges in linking meteorites to specific types of asteroids because meteorite taxonomies have been developed using different techniques than telescopic asteroid surveys. For example, it is not clear how many distinct asteroids we have samples of (Burbine et al., 2002), how strongly the atmosphere biases the collection against weak material like that found on Ryugu or Bennu (e.g., Bischoff et al., 2022), and whether there are unique compositions represented in the asteroids but not captured in the sample collection (Hasegawa et al., 2021; Kurokawa et al., 2022). Nevertheless, progress is continually being made (DeMeo et al., 2022) and many firm links (e.g., S-types and ordinary chondrites; Nakamura et al., 2011) and tentative links (e.g., A-types and brachinites; Sanchez et al., 2014) have been established.

In this work, meteorite compositions were sourced from a variety of literature values. Compositions for Fig. 2 were harvested from MetBase (Koblitz, 2003), a database compiled from primary literature sources. The advantages of using this compilation are the breadth of data available and built-in search tools, but there are some drawbacks. Datapoints are not easily traced back to literature provenance in MetBase, and data entry errors and outliers are present. Therefore, only primary sources were used for the more rigorous analysis of certain downselected elements. Table 1 lists data sources for PGMs; sources for

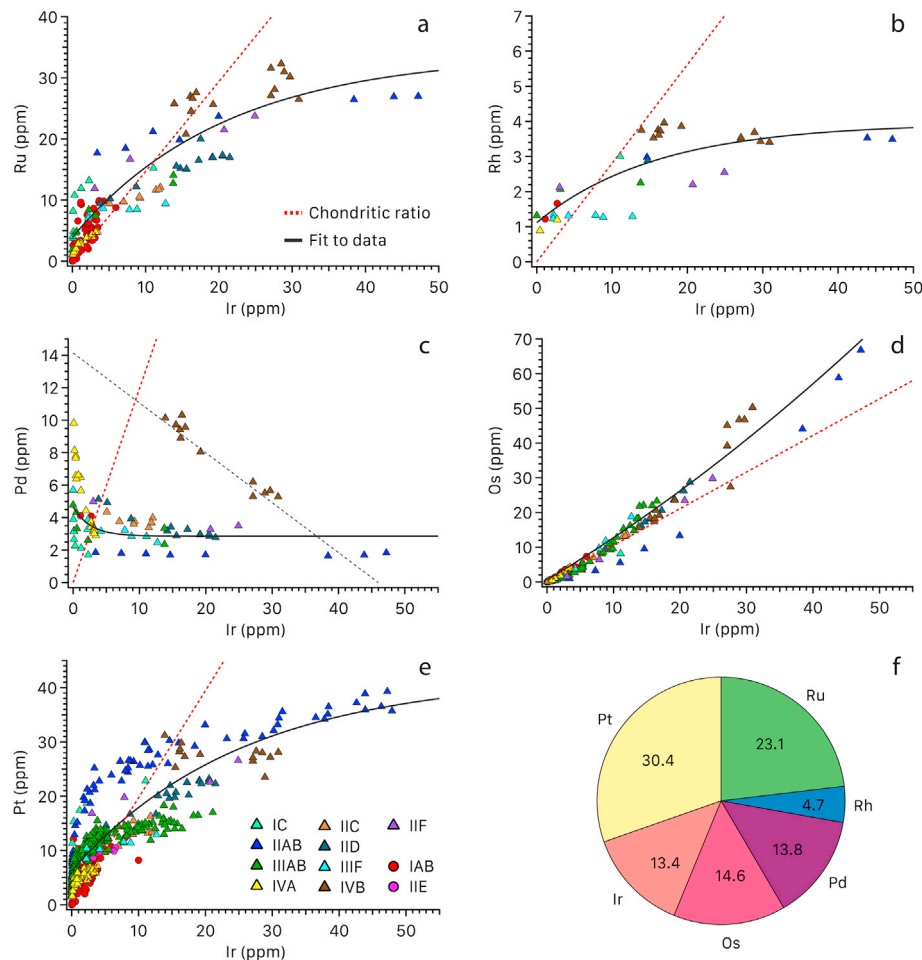


Fig. 3. Trends of PGMs vs. Ir concentrations in different iron meteorite groups (see legend in plot (e)). Black lines show best fits to data, and dashed red lines show chondritic ratios (Lodders, 2003). (f) Average breakdown of PGMs using the statistical sampling.

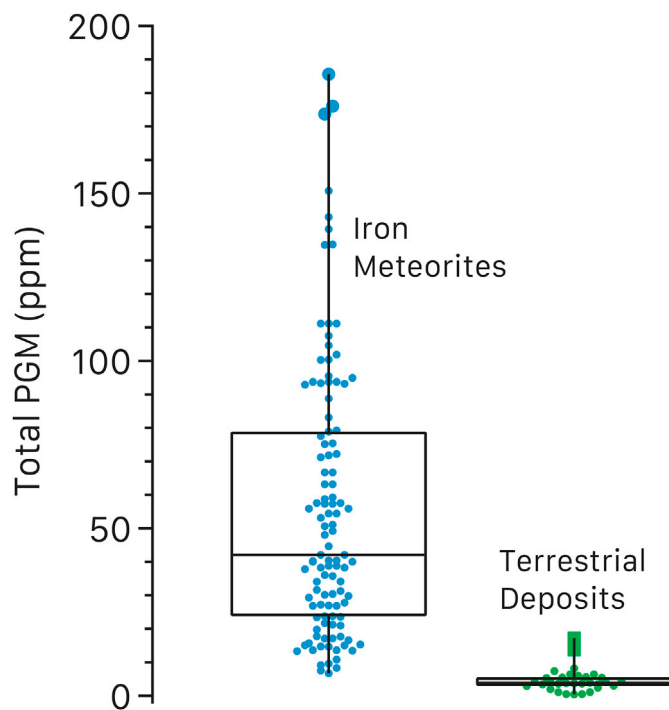


Fig. 4. Distributions of total PGMs grade in the statistical sampling of iron meteorites compared to terrestrial ores.

Table 2

Percentiles of total PGM grade from the statistical sampling of iron meteorites compared to terrestrial deposits.

Percentile	PGMs (iron meteorites), ppm	PGMs (terrestrial deposits), ppm
10th	14.70	1.07
20th	20.75	2.39
30th	27.05	3.40
40th	34.77	3.62
50th	40.78	3.86
60th	52.88	4.19
70th	63.48	5.40
80th	91.23	6.00
90th	107.86	7.36

structural/photovoltaic metals are identified in Tables 3 and 4.

2.2. Statistical sampling of iron meteorites

For the iron meteorites we are aiming for a robust picture of PGM contents, but many of the meteorite analyses from Table 1 are missing certain PGMs. In addition, the number of measured samples differs between iron meteorite groups, likely in part due to different sizes of their respective parent bodies. The compiled PGM dataset (see Supplementary Material) contains 141 measurements for Ru, 40 for Rh, 81 for Pd, 182 for Os, 618 for Ir, and 548 for Pt. We removed duplicate analyses of the same meteorite from different sources, keeping those analyses with more PGMs measured and those measured using INAA. To fill in missing values, we used regressions against Ir for the other 5 PGMs (see Fig. 3). To compare with terrestrial deposits, we used a statistical sampling approach from the compiled PGM data. We assumed each iron meteorite group comes from a single parent body, which is a good approximation for most groups except the IABs (Worsham et al., 2016). We selected 10 randomly chosen meteorites from each group, which the choices weighted such that meteorites with measurements of the most PGMs were chosen first. This procedure was repeated 100 times to build up a statistical picture.

2.3. Baseline values from terrestrial ores

Terrestrial ore grades from currently operating mines provide the best baseline to compare with elemental concentrations on asteroids. Ore grades (i.e., concentrations) are typically reported in g/t (equivalent to ppm by mass) or weight percent (wt.%). Grade is a proxy for the energy or cost to extract a pure element or mineral from the raw ore, and energy costs go up exponentially as grades decline (Calvo et al., 2016). In most countries, publicly owned mining companies are required to report grades and total amounts for a given deposit or project. Usually these are classified using a system like JORC (JORC, 2012) that separates inferred, indicated, and measured resources, and probable and proven reserves. Terrestrial ore grades for the detailed comparisons in this work were taken from such reports. For the cursory comparisons in Fig. 2, a broader range of literature and online sources were used to gather typical or maximum ore grades for 83 elements on Earth.

3. Results

3.1. Survey of elements on asteroids

Only a small minority of chemical elements have concentrations in at least one meteorite (and therefore asteroid) of any type that approach or exceed terrestrial ore grades: Ir, Ru, Os, Ni, Pt, Rh, Co, O, Pd, Fe, and Mg (see Supplementary Material). Fig. 2 color codes the ratio of maximum concentrations likely found on asteroids to concentrations in high-grade ores or deposits on Earth (note the log scale). For in-space use, this ratio is a crude estimate of how much it makes sense to launch a certain element versus sourcing it in space, or how far in the future we may transition from the former to the latter. For return-to-Earth, the ratio highlights potential candidate targets, but the amount of ore mined per year must be considered too. As an example, Fe, Ni, and Co are more concentrated in certain asteroids than the best terrestrial ores, but the world collectively mines ~2.4 billion tons of iron ore per year, 2.7 million tons of nickel ore, and 170 thousand tons of cobalt ore (U.S. Geological Survey, 2022). Therefore, returning these metals to Earth is a non-starter.

Most elements are more than $\sim 100 \times$ more concentrated in terrestrial deposits (including the atmosphere) compared to asteroids: meteorites of all types are particularly depleted in the noble gases, light rare earths, Be and B, nuclear fuels U and Th, and post-transition metals. Just below the breakpoint (asteroid concentration = terrestrial ores) are Ge, Au, Si and Al. In this work, the PGMs are explored as potential return-to-Earth resources, and Fe, Mg, Si and Al as structural/photovoltaic metals for in-space use. Ni, Co, Ge, and Au are judged to be marginal and are not discussed further, and O is relevant for in-space propellant which has been covered by other authors (Jedicke et al., 2018; Rivkin and DeMeo, 2019; Colvin et al., 2020).

3.2. Breaking down the PGMs

While PGMs in asteroids have been described in previous work, the data now available make these numbers worth revisiting. Kargel (1994) examined Ir contents from a compilation of iron meteorites and ordinary chondrites, then applied chondritic ratios to infer the concentration of the other PGMs as well as Au. For example, if an iron meteorite has 40 ppm Ir and the ratio of Ru/Ir is 1.471 in CI carbonaceous chondrites (Lodders, 2003), then the Kargel approach predicts 58.84 ppm Ru in the same meteorite. Now that better data are available from LA-ICP-MS and the more accurate ID-ICP-MS and INAA (Table 1), we should use actual measurements of Ru rather than relying on these inferences. The Kargel approach led to estimates of over 300 ppm total PGM which are no longer supported by measurements of the other elements. Based on our regressions below (see Figs. 3 and 4), the IAB Avce at ~230 ppm total PGM (Wasson et al., 2007) represents about the highest value that can be expected. Note also the Ir values reported by Elvis (2014) as up to 100 ppm (which would imply as much as 700 ppm total PGM) seem to be a

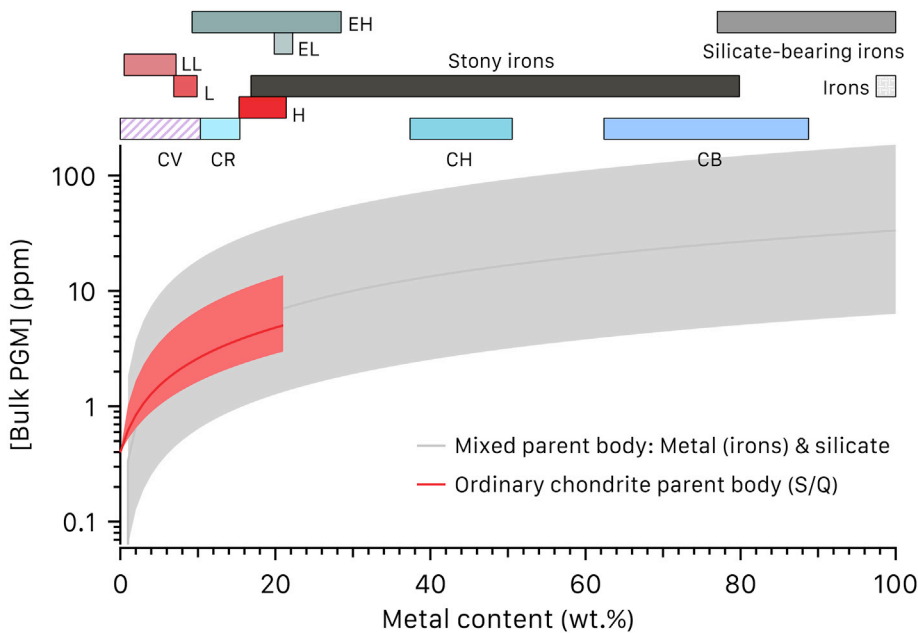


Fig. 5. Top: ranges of metal contents in different meteorite classes (Stony irons: Mason and Jarosewich, 1973; Silicate-bearing irons: McCoy et al., 1996; LL, L, H: Dunn et al., 2010; EH, EL: Weisberg and Kimura, 2012; CR: Howard et al., 2015; CV: Bonal et al., 2020; CH, CB: Weyrauch et al., 2021). Bottom: linear mixing models from the statistical sampling of PGMs for X-complex (gray) and S/Q-type asteroids (red) showing how PGM grade may vary as a function of total metal content (see Supplementary Material). Only at the highest fractions of metal would asteroids reach the types of grades shown in Fig. 4.

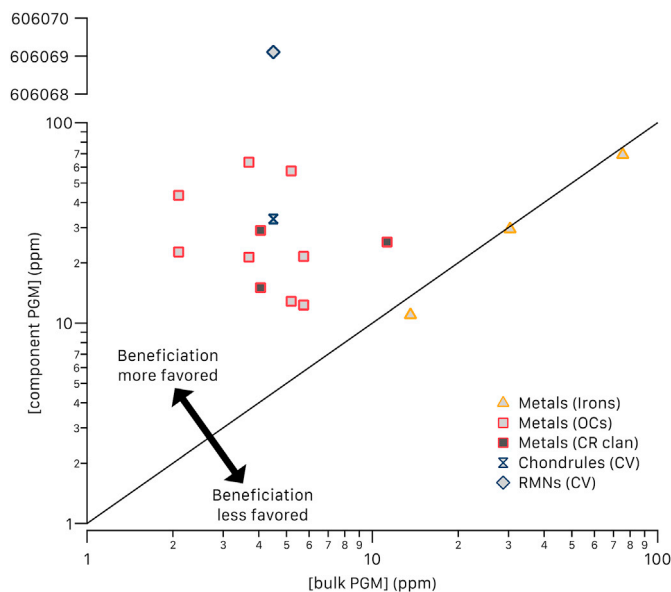


Fig. 6. PGM grades in individual meteorite components (metal grains, chondrules, etc.) plotted against the PGM grade in the bulk meteorite (Irons: Petaev and Jacobsen, 2004; CR metal: Horan et al., 2003; Weyrauch et al., 2021; van Kooten et al., 2022; Chondrules: Archer et al., 2014; RMNs: Daly et al., 2017; OC metal: Okabayashi et al., 2019; Horan et al., 2009). Components falling above the 1:1 solid black line may be suitable for mineral processing/beneficiation to enrich the PGM grade. Note the large gap along the y-axis where RMNs fall.

misreading of Kargel (1994), who report up to 50 ppm Ir in the richest irons as is still supported by the data. For example, Avce has 59.5 ppm Ir (Wasson et al., 2007) and Negrillos has 47.2 ppm (Petaev and Jacobsen, 2004).

Updated measurements demonstrate PGMs are not present in chondritic ratios with respect to Ir across different iron meteorite groups. Fig. 3 shows our compilation (Table 1; Supplementary Material) where Ir and at least one of the other 5 PGMs are available from the same meteorite sample. On each graph a best fit to the data is plotted with a solid black line, and the linear chondritic ratio from CI carbonaceous

chondrites (Lodders, 2003) in a dashed red line. As Fig. 3 shows, the trends versus Ir are generally only linear at very low Ir values. Ru, Rh, and Pt roll over at higher Ir values (Fig. 3a, b, e), such that using chondritic ratios would significantly overestimate PGM grades at the high end of Ir. Pd is inversely correlated with Ir (Fig. 3c), with the IVB irons offset on their own trendline. Os is the only PGM that monotonically increases with increasing Ir (Fig. 3d), showing slightly superchondritic ratios.

Each of the 6 PGMs is not equally abundant in iron meteorites. Fig. 3f shows the average breakdown of PGM content from the statistical sampling method described above (§2.2). Pt and Ru account for more than half the total budget. Ir, Os, and Pd are present in lower amounts, and Rh is by far the least abundant. The breakdown in Fig. 3 by meteorite subgroup on a per-PGM basis is useful if a particular PGM is being targeted rather than the full suite.

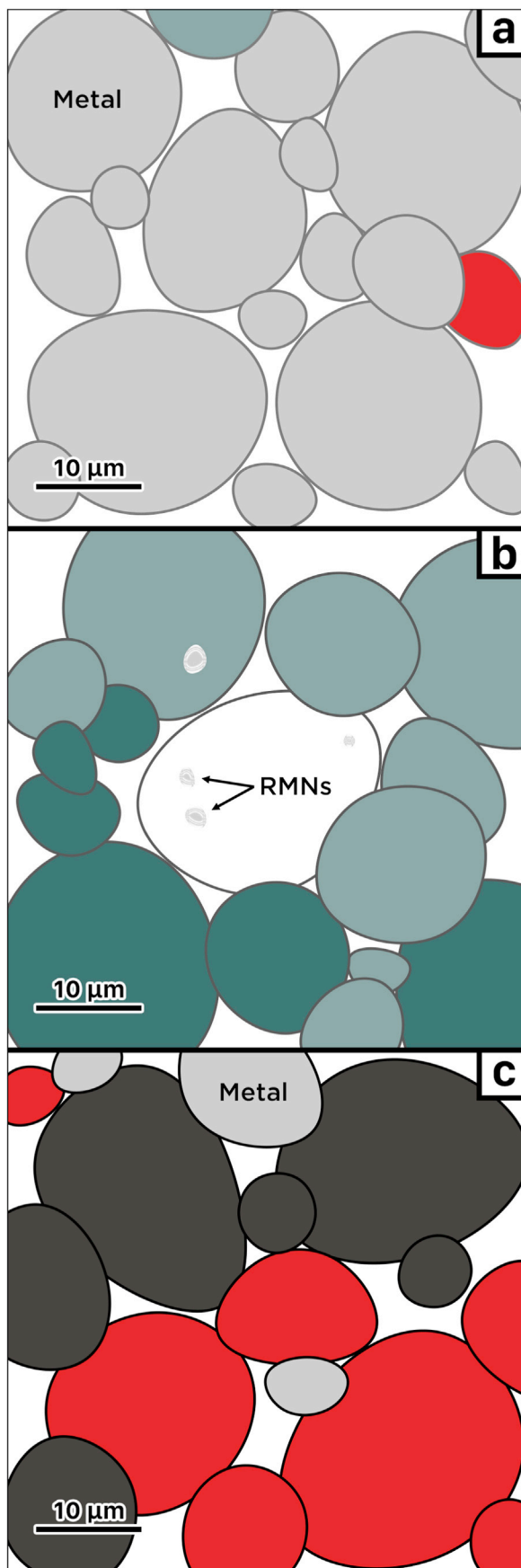
3.3. PGMs compared with terrestrial values

The PGMs appear to be more concentrated in some space materials than terrestrial ores (Fig. 2), and this is borne out by a more rigorous comparison. Fig. 4 shows total PGM grades from the statistical sampling method. Also shown for comparison are ore grades from terrestrial mining projects and exploration targets (see Supplementary Material). Almost every iron meteorite has higher combined PGM concentrations than any terrestrial deposit, except for the Sibanye-Stillwater mine in Montana that exceeds some of the lowest-grade irons. Table 2 presents the percentiles derived from this analysis, which should be seen as an up-to-date improvement on the Kargel (1994) study.

4. Discussion

4.1. Potential return-to-earth elements: PGMs

Platinum group metals remain the only likely prospect for elements returned to Earth from asteroids because of their high value, high grades in asteroid materials, and low amounts mined per year on Earth. As mentioned above, some PGMs have exceedingly high market values and are only mined in single- or double-digit tons per year. There could be a near-term case to return these metals if SpaceX Starship launch costs come down and ore grades continue to decline on Earth (Northey et al., 2014; Calvo et al., 2016). Other factors could increase the economic case, for example more scrutiny in Environmental, Social, and Governance



(caption on next column)

Fig. 7. Hypothetical regoliths of different asteroids and strategies for targeting PGMs. (a) A metal-rich (but not 100% pure metal) asteroid where the bulk material is suitable for directly extracting certain elements. (b) An asteroid rich in CAIs (perhaps an L- or K-type) from which micron-sized RMNs could possibly be separated. (c) A metal bearing asteroid (including some E-, S-, Q-types, and the metal-poor end of the X-complex) from which larger grains of metal that host most of the PGMs could be separated more readily.

(ESG) issues including expanded carbon taxes that make mining companies responsible for costs currently borne by broader society (e.g., Van Der Zee et al., 2013).

The data presented in Figs. 3 and 4 assume there are asteroids made of pure metal, but other possibilities should be explored given our current understanding of M-type asteroids. Previous work like Kargel (1994) and Lewis (1996) assumed M-types are solid chunks of iron-nickel metal from which the iron meteorites are derived. Years of density, spectroscopy, and radar reflectivity studies (e.g., Shepard et al., 2015) suggest the picture is more complicated. While some X-Complex bodies are enriched in metals as evidenced by high bulk densities and radar albedos, the pure metallic asteroid is now seen as an extreme endmember that may not exist in practice (e.g., Elkins-Tanton et al., 2022). Other materials including metal-rich enstatite chondrites (e.g., EH), ordinary chondrites (e.g., H), carbonaceous chondrites (e.g., CH, CB), and stony irons (pallasites, mesosiderites) could also have X-Complex parent bodies, a classification which may represent a continuum between metal-poor and metal-rich objects. Given the uncertainties involved with different remote sensing techniques, a spacecraft sent to an X-Complex asteroid is likely to encounter an unknown proportion of metals and silicates. The PGM ranges in Fig. 4 and percentiles in Table 2 should therefore be interpreted as upper values because they represent 100% metal content. Fig. 5 shows how total PGM grades may vary for metal contents <100% using mixing models from two hypothetical cases: an iron meteorite parent body with some fraction of silicates, and an ordinary chondrite parent body. Even if an object has high Fe-Ni metal content (i.e., plots to the right of Fig. 5), there is no known way to remotely identify where an asteroid falls along the wide distributions of PGM grades shown in Fig. 4. The complete range of percentiles should be kept in mind, and the 50th percentile values (Table 2) provide a better expectation than the 90th percentiles as in Kargel (1994).

Meteorite studies highlight other types of asteroid materials that host phases enriched in PGMs, and these could be targeted by going to objects other than X/M-types. Metal grains and matrix material are present in varying proportions in many different chondritic and achondritic meteorites. When metals and bulk meteorites have both been measured for PGMs from the same samples, the metal grains have been found to host the vast majority of the PGM budget (e.g., Horan et al., 2009), such that separating the metal out would greatly increase the PGM grade above that of the bulk material. In the most extreme case, refractory metal nuggets (RMNs) found mostly in type-3 CV/CO chondrites can reach weight percent levels of PGMs (Daly et al., 2017). These RMNs are preferentially hosted in calcium aluminum inclusions (CAIs), and L-type asteroids believed to be rich in CAIs (Devogèle et al., 2018) could be a promising source. Sunshine et al. (2008) suggest L-types may consist of up to 30% CAIs. However, RMNs are extremely small (micron to sub-micron; Daly et al., 2017), which is about the limit of even the most sensitive mineral processing/beneficiation techniques. Gravity separation using autogenous heavy liquids is an option and could use clays in the matrix material of CI or CM-like material. However, RMNs have not been reported from CI or CM chondrites: this could be due to a general lack of CAIs in these meteorite types (Rubin, 2018), but if CAIs were accreted and destroyed by aqueous alteration the fate of any RMNs remains in question.

Plotting component grades (e.g., metal grains, RMNs) against the bulk material grade can reveal different strategies for processing asteroidal materials to extract precious metals. Fig. 6 plots PGM grades for individual components in cases where the PGM concentration of the bulk

Table 3

Bulk concentrations of Fe (oxidized), Mg, Al, and Si in examples from meteorites compared to mean CI concentrations from [Palme et al. \(2014\)](#).

Element	Mean CI concentration (wt.%) ^a	Exemplar meteorite (type)	Bulk concentration in that meteorite (wt.%)	Promising asteroid type(s)
Fe	18.88	Lewis Cliff (LEW) 87009 ^b (CK6)	22.50	Any
Mg	9.54	Allan Hills (ALH) 84136 ^b (Ureelite)	24.14	A
Al	0.84	Serra de Magé ^c (Eucrite)	10.16	V
Si	10.70	Northwest Africa (NWA) 11119 ^d (Achondrite-ung)	25.00	Differentiated

^a From [Palme et al. \(2014\)](#).

^b [Jarosewich \(2006\)](#).

^c [Ma and Schmitt \(1979\)](#).

^d [Srinivasan et al. \(2018\)](#).

material is also available for that meteorite. On such a plot, components that fall to the upper left of the 1:1 line could be enriched by mineral processing where it is feasible to do so. As expected, iron meteorite samples plot nearly on the 1:1 line because almost the whole meteorite is Fe–Ni metal. If a truly metal-rich asteroid is found, its regolith could be processed directly without any beneficiation. All the other components (metal grains, chondrules, RMNs) fall above the line, indicating it could make sense to try and separate them from the bulk material before extracting specific elements. For example, regoliths of S- and Q-type asteroids linked to ordinary chondrites ([Nakamura et al., 2011](#)) may have both free metal grains and metal-silicate middlings in their regoliths, and mineral processing would enrich the metal content and therefore the PGM grade. The same is true for RMNs which plot extremely high along the y-axis in [Fig. 6](#), but a path to effective separation is more dubious. These three strategies for targeting different components are illustrated graphically in [Fig. 7](#).

4.2. Metals for in-space use: Fe, Mg, Al, Si

The other elements with high ratios in [Fig. 2](#) include base metals like Si and Al that will not be economically returned to Earth but instead have immense potential for in-space use. Here the speciation of these elements becomes more important. PGMs are alloyed in the metallic phases kamacite, taenite, and tetrataenite and are present in +0 or native oxidation states. Mg, Al, and Si are found nearly exclusively in oxidized forms within silicates, oxides, and carbonates (among others) and would

need to be chemically reduced using a process such as molten regolith electrolysis to extract them as metals. Fe falls in between: it is present in asteroids as Fe³⁺ (e.g., in magnetite), Fe²⁺ (e.g., in olivine, pyroxene) and Fe⁰ (e.g., Fe–Ni metal as discussed above). Metal-poor asteroids will still have significant levels of total Fe but much of this would need to be reduced. For example, Orgueil has no metal, but a total Fe content of 18.9 wt% ([Jarosewich, 1990](#)).

Parent bodies of metal-rich meteorites are clear destinations for precious metals, but it is not as obvious which types of asteroids we should go to when targeting these other bulk metals. The geochemical behavior of Fe, Mg, Al and Si during geological processes and the compilation that went into [Fig. 2](#) provide a starting guide for identifying the types of meteorite materials with the highest concentrations of these elements. [Table 3](#) shows the concentration of these elements in average CI chondrites taken to be “bulk solar system” ([Lodders, 2003](#); [Palme et al., 2014](#)), and concentrations in specific meteorites that have the some of the highest probable values. In this table, the row for Fe focuses only on oxidized Fe; if metallic Fe were included then iron meteorites would reach nearly 100% (except the silicate-bearing IABs and IIEs). [Table 4](#) lists concentrations of Fe, Mg, Al, and Si in specific meteorite components where the bulk concentration is also available for that meteorite.

No meteorites greatly exceed the CI value for bulk oxidized Fe, but the CK6 chondrite Lewis Cliff (LEW) 87009 had the highest value in a cursory survey ([Table 3](#)). This suggests almost any asteroid can be a source of Fe if it can be chemically reduced, which is somewhat comforting given that it can be difficult to definitively identify metallic Fe on asteroids through remote sensing using the most common technique of reflectance spectroscopy (but see [Harris and Drube, 2014](#)). Silicate phases like olivine and pyroxene are not strongly enriched in Fe compared to bulk meteorites, but the Fe oxide magnetite is ([Table 4](#)) and is relatively abundant in aqueously altered type 1 and 2 carbonaceous chondrites (CCs). This could be relevant for processing slag after extracting water from clays, and magnetite is advantageous because it is one of the main terrestrial iron ores (can use the same extraction techniques) and it can be magnetically manipulated/separated.

The chondritic abundance of Mg is only about half that of Fe by mass ([Lodders, 2003](#); [Palme et al., 2014](#)), but certain differentiated or partially differentiated asteroids contain significant enrichments above this value. These include the urelites ([Table 3](#)), and brachinites abundant in Mg-rich olivine with potential links to the never-visited A-type asteroids. In addition to the olivine itself, phases like Mg-spinel on type-3 CCs and magnesite on hydrated CCs are modestly enriched in Mg above the bulk ([Table 4](#)). It is not clear whether this is enough to warrant separating these phases through mineral processing. Mg may be the most difficult element to extract as a pure metal from asteroid materials of those discussed in this section.

Al contents are universally low in undifferentiated bodies but can reach reasonable amounts in achondritic crusts ([Usui and McSween, 2007](#)). The eucrites from the Howardite, Eucrite, Diogenite (HED) suite

Table 4

Concentrations of Fe, Mg, Al, and Si in specific meteorite components.

Element	Meteorite (type)	Component	Concentration in component (wt.%)	Component to bulk ratio	Asteroid link(s)
Fe	(CI)	Magnetite	72.36 ^a	3.8	C
Mg	Orgueil (CI)	Magnesite	17.55 ^b	1.8	C
Mg	Allende (CV3)	Spinel	15.99 ^c	1.1	K
Mg	Eagles Nest (Brachinite)	Olivine	21.32 ^d	1.3	A
Al	Allende (CV3)	Spinel	35.97 ^c	21.0	K
Al	Allende (CV3)	Hibonite	47.37 ^c	27.7	K
Al	Serra de Magé	Plagioclase	17.47 ^e	1.7	V
Si	NWA 11119 (Achondrite-ung)	Silica	45.97 ^f	1.6	?

^a Idealized formula.

^b [Johnson and Prinz \(1993\)](#).

^c [Kornacki and Wood \(1985\)](#).

^d [Swindle et al. \(1998\)](#).^e [Ma and Schmitt \(1979\)](#).

^f [Srinivasan et al. \(2018\)](#).

Table 5

Asteroid classes from the [Mahlke et al. \(2022\)](#) taxonomy, plausible meteorite analogs, and potential grades and relevant components for both precious and base metals.

Asteroid Class	Meteorite Analog(s)	Precious metals	Base metals
Z, D, P, Ch, C, B	Interplanetary dust particles, carbonaceous chondrites, some unsampled?	Low grades; RMNs possible; some could have metal grains	CI-like concentrations of Fe, Mg, Al, Si
E	Aubrites, enstatite chondrites/achondrites	Low to moderate grades; some metal grains and/or matrix	Higher in Si than CIs
M	Irons, stony irons, enstatite chondrites(?), CH/CB(?)	Moderate to high grades; metal grains and/or matrix that could dominate in most metal-rich examples	Metal-rich examples will be extremely high in Fe and depleted in Mg, Si and Al
L	CAI-rich chondrites?	Low to moderate bulk grades; if rich in CAIs, should also be rich in RMNs	Likely enriched in Al above CI
K	CV, CO, CK chondrites	Low grades; some metal grains and RMNs possible	No notable enrichments/depletions
A	Brachinites, R-chondrites, mesosiderites	Low grades; few enriched components	Enriched in Mg and Si above CIs
V	HEDs	Extremely low grades; few enriched components	Enriched in Al, Si and Mg, and depleted in Fe compared to CIs
S, Q	Ordinary chondrites	Low to moderate grades; some free metal grains	Metal-rich examples higher in Fe than CIs

are the most enriched in terms of bulk Al, with Serra de Magé having a particularly high concentration of 19.2 wt% Al_2O_3 ([Table 3](#)); V-type asteroids including Vesta are promising targets to find this material. Minerals like hibonite and spinel found in CAIs have quite extreme Al enrichments above the bulk ([Table 4](#)).

Si has similar chondritic values as Mg and is also enriched to nearly the same extent in certain bulk meteorites. The rare and only recently studied evolved igneous compositions represented by Graves Nunataks (GRA) 06129 ([Shearer et al., 2011](#)) and Northwest Africa (NWA) 11119 ([Srinivasan et al., 2018](#)) have quite high silica contents amongst the meteorites ([Table 3](#)), but it is not clear what types of parent bodies these are linked to. Otherwise, the HEDs (especially diogenites) reach quite high total Si contents ([Jarosewich, 1990](#)) and have a more straightforward asteroid connection. The pure silica itself in a meteorite like NWA 11119 likely has the highest Si content of any meteorite mineral ([Table 4](#)); garden variety silicates are an alternative.

[Table 5](#) summarizes the potential for the different asteroid classes from [Mahlke et al. \(2022\)](#)'s taxonomy to be a source of both precious and base metals, including the likely components found within those asteroids.

4.3. Use cases for asteroid metals

Use cases and architectures will differ significantly from element to element for the metals considered here. For elements like Rh and Ir that have extremely high market values and are mined in minute amounts on Earth, there could be an incipient case to return these metals and sell them into existing commodity markets. Flooding the market with space-derived sources of these materials would obviously lower prices ([Kargel, 1994](#)), but there are likely diverse applications where PGMs offer advantages in material properties over other metals but are not currently

being used because they cost too much. On the other hand, elements like Al and Si will solely be used for in-space applications. Evidence for emerging interest in metals and manufacturing in space includes: (1) a set of NASA contracts to Redwire Corporation for a series of missions called On-Orbit Servicing, Assembly and Manufacturing (OSAM) and Archinaut One, part of which involves building beams in orbit; (2) The DARPA NOM4D program exploring technologies that use space materials to manufacture structures including megawatt-class solar arrays and radio frequency reflector antennas; and (3) Neumann Space developing an arc thruster that can use any conductive material as fuel, including metals like Al. Future projects could include commercial space stations or more ambitious space habitats, space-based solar power, or a planetary sunshade at Sun-Earth Lagrange 1 ([Jehle et al., 2020](#)) that would involve megatons of space materials, mostly metals.

4.4. Processing considerations

Extracting pure elements or compounds from asteroid material will not be straightforward, and flowsheets will need to be developed that mimic those used on Earth. In terrestrial mining, flowsheets are used to describe the sequence of unit processes to take the bulky raw ore (which cannot be used as-is) and turn it into a fine-grained concentrate suitable for smelting or other extraction methods. The first steps in terrestrial flowsheets usually involve comminution and size sorting. Many early asteroid mining concepts and research came before we recognized most small and medium sized asteroids are rubble piles ([Harris, 1996](#); [Sánchez and Scheeres, 2014](#)). Additionally, new data from Hayabusa2 and OSIRIS-REX emphasize the extremely weak, fluffy nature of the boulders and surface materials with microporosity values up to and exceeding 50% ([Grott et al., 2019](#)), at least for CCs. Textures of metal-rich asteroid surfaces remain to be investigated. These characteristics will challenge technologies used for proximity operations, landing, anchoring, excavating, conveying, and processing asteroid materials. However, weak porous materials should require extremely low energy to crush, which could favor architectures that use mechanical energy rather than solar to comminute material. For concentrating valuable minerals, terrestrial techniques that use fluids and gravity will have to be re-thought; centrifugal forces may become quite important. It will be difficult to sort value minerals from gangue in undifferentiated asteroids where matrix grain sizes are commonly submicron, but on the other hand this could make transporting bulk material with electromagnetic fields quite straightforward. Newly emerging architectures for extracting metals from asteroids should consider the complete path from raw asteroid regolith to finished products, especially given more nuanced recent thinking on M-type asteroids. The data and strategies presented here can be a starting point to develop asteroid-specific flowsheets.

5. Conclusions

Asteroids are a promising source of metals in space, and this promise will mostly be unlocked in the main belt where the Accessible Mining Volume of bodies greatly exceeds that of the terrestrial planets and moons. Metals on asteroids can be roughly divided between precious metals—especially the PGMs—which could potentially be returned to Earth and sold into existing commodity markets, and base metals like Al and Si used for structural purposes (beams, trusses, etc.) and for solar photovoltaic panels. There are only a small handful of elements whose maximum concentrations in plausible asteroid materials exceed the best ores on Earth. Among these elements, the total concentration of PGMs in iron meteorites varies between ~6 and 230 ppm, higher than almost all terrestrial ores. However, previously reported values up to 300 ppm (or 700 ppm) based on extrapolating chondritic ratios are not supported by actual measurements of PGMs. Newer understandings of M-type asteroids move away from the idea of monolithic mountains of metal and toward more complex silicate-metal mixtures, such that meteorite metals provide what are likely maximum values for siderophile elements like

PGMs. Mineral processing/beneficiation can upgrade concentrations of these elements by targeting metal grains, or components like refractory metal nuggets on different asteroid types such as L-types. Most asteroids contain modest concentrations of the structural/photovoltaic metals Fe, Mg and Si, with much lower Al, all in oxidized forms requiring chemical reduction. Certain asteroid types and components in their regolith are more enriched, for example magnetite as a source of oxidized Fe or hibonite as a source of Al. Rare, silica-rich meteorites are an intriguing source of Si but have no clear asteroid links.

Author statement

Kevin Cannon: Conceptualization, Methodology, Investigation, Writing, Visualization **Matt Gialich:** Conceptualization, Review, Supervision. **Jose Acain:** Conceptualization, Review, Supervision.

Declaration of competing interest

The authors declare the following financial interests/personal relationships which may be considered as potential competing interests: Kevin Cannon reports financial support was provided by AstroForge Inc.

Data availability

In attached supplemental

Acknowledgements

The authors would like to thank an anonymous reviewer for their thorough and constructive comments that significantly improved the manuscript.

Appendix A. Supplementary data

Supplementary data to this article can be found online at <https://doi.org/10.1016/j.pss.2022.105608>.

References

- Archer, G.J., Ash, R.D., Bullock, E.S., Walker, R.J., 2014. Highly siderophile elements and 187Re-187Os isotopic systematics of the Allende meteorite: evidence for primary nebular processes and late-stage alteration. *Geochim. Cosmochim. Acta* 131, 402–414. <https://doi.org/10.1016/j.gca.2013.12.032>.
- Bischoff, A., Bannemann, L., Decker, S., Ebert, S., Haberer, S., Heitmann, U., Horstmann, M., Klemm, K.I., Kraemer, A., Lentfort, S., Patzek, M., Storz, J., Weyrauch, M., 2022. Asteroid 2008 TC 3, Not a Polymict Ureilitic but a Polymict C1 Chondrite Parent Body? Survey of 249 Almahata Sitta Fragments. *Meteorit. & Planetary Scien. maps*, 13821. <https://doi.org/10.1111/maps.13821>.
- Bonal, L., Gattacceca, J., Garenne, A., Eschrig, J., Rochette, P., Krämer Ruggiu, L., 2020. Water and heat: new constraints on the evolution of the CV chondrite parent body. *Geochim. Cosmochim. Acta* 276, 363–383. <https://doi.org/10.1016/j.gca.2020.03.009>.
- Burbine, T.H., McCoy, T.J., Meibom, A., Gladman, B., Keil, K., n.d. Meteoritic parent bodies: their number and identification, in: *Asteroids III*.
- Calvo, G., Mudd, G., Valero, Alicia, Valero, Antonio, 2016. Decreasing ore grades in global metallic mining: a theoretical issue or a global reality? *Resources* 5, 36. <https://doi.org/10.3390/resources5040036>.
- Campbell, A.J., Humayun, M., 2005. Compositions of group IVB iron meteorites and their parent melt. *Geochim. Cosmochim. Acta* 69, 4733–4744. <https://doi.org/10.1016/j.gca.2005.06.004>.
- Chabot, N.L., Zhang, B., 2022. A revised trapped melt model for iron meteorites applied to the IIIAB group. *Meteoritics Planet. Sci.* 57, 200–227. <https://doi.org/10.1111/maps.13740>.
- Colvin, T.J., Crane, K., Lal, B., 2020. Assessing the economics of asteroid-derived water for propellant. *Acta Astronaut.* 176, 298–305. <https://doi.org/10.1016/j.actaastro.2020.05.029>.
- Daly, L., Bland, P.A., Dyl, K.A., Forman, L.V., Evans, K.A., Trimby, P.W., Moody, S., Yang, L., Liu, H., Ringer, S.P., Ryan, C.G., Saunders, M., 2017. In situ analysis of Refractory Metal Nuggets in carbonaceous chondrites. *Geochim. Cosmochim. Acta* 216, 61–81. <https://doi.org/10.1016/j.gca.2016.11.030>.
- DeMeo, F.E., Binzel, R.P., Slivan, S.M., Bus, S.J., 2009. An extension of the Bus asteroid taxonomy into the near-infrared. *Icarus* 202, 160–180. <https://doi.org/10.1016/j.icarus.2009.02.005>.
- DeMeo, F.E., Burt, B.J., Marsset, M., Polishook, D., Burbine, T.H., Carry, B., Binzel, R.P., Vernazza, P., Reddy, V., Tang, M., Thomas, C.A., Rivkin, A.S., Moskovitz, N.A., Slivan, S.M., Bus, S.J., 2022. Connecting asteroids and meteorites with visible and near-infrared spectroscopy. *Icarus* 380, 114971. <https://doi.org/10.1016/j.icarus.2022.114971>.
- Devogèle, M., Tanga, P., Cellino, A., Bendjoya, Ph, Rivet, J.-P., Surdej, J., Vernet, D., Sunshine, J.M., Bus, S.J., Abe, L., Bagnulo, S., Borisov, G., Campins, H., Carry, B., Licandro, J., McLean, W., Pinilla-Alonso, N., 2018. New polarimetric and spectroscopic evidence of anomalous enrichment in spinel-bearing calcium-aluminium-rich inclusions among L-type asteroids. *Icarus* 304, 31–57. <https://doi.org/10.1016/j.icarus.2017.12.026>.
- Dunn, T.L., Cressley, G., McSween Jr., H.Y., McCoy, T.J., 2010. Analysis of ordinary chondrites using powder X-ray diffraction: 1. Modal mineral abundances. *Meteoritics Planet. Sci.* <https://doi.org/10.1111/j.1945-5100.2009.01011.x>.
- Elkins-Tanton, L.T., Asphaug, E., Bell, J.F., Bierson, C.J., Bills, B.G., Bottke, W.F., Courville, S.W., Dobb, S.D., Jun, I., Lawrence, D.J., Marchi, S., McCoy, T.J., Merayo, J.M.G., Oran, R., O'Rourke, J.G., Park, R.S., Peplowski, P.N., Prettyman, T.H., Raymond, C.A., Weiss, B.P., Wiczorek, M.A., Zuber, M.T., 2022. Distinguishing the origin of asteroid (16) Psyche. *Space Sci. Rev.* 218, 17. <https://doi.org/10.1007/s1214-022-00880-9>.
- Elvis, M., 2014. How many ore-bearing asteroids? *Planet. Space Sci.* 91, 20–26. <https://doi.org/10.1016/j.pss.2013.11.008>.
- Grott, M., Knollenberg, J., Hamm, M., Ogawa, K., Jaumann, R., Otto, K.A., Delbo, M., Michel, P., Biele, J., Neumann, W., Knapmeyer, M., Kührt, E., Senshu, H., Okada, T., Helbert, J., Maturilli, A., Müller, N., Hagermann, A., Sakatani, N., Tanaka, S., Arai, T., Mottola, S., Tachibana, S., Pelivan, I., Drube, L., Vincent, J.-B., Yano, H., Pilonet, C., Matz, K.D., Schmitz, N., Koncz, A., Schröder, S.E., Trauthan, F., Schlotterer, M., Krause, C., Ho, T.-M., Moussi-Soffys, A., 2019. Low thermal conductivity boulder with high porosity identified on C-type asteroid (162173) Ryugu. *Nat. Astron.* 3, 971–976. <https://doi.org/10.1038/s41550-019-0832-x>.
- Gunn, G., 2013. Platinum-group metals. In: Gunn, G. (Ed.), *Critical Metals Handbook*. John Wiley & Sons, Oxford, pp. 284–311. <https://doi.org/10.1002/9781118755341.ch12>.
- Harris, A.W., 1996. The rotation rates of very small asteroids. In: *Evidence for "Rubble Pile" Structure*, 27, p. 493.
- Harris, A.W., Drube, L., 2014. How to find metal-rich asteroids. *APJ (Acta Pathol. Jpn.)* 785, 14. <https://doi.org/10.1088/2041-8205/785/1/L4>.
- Hasegawa, S., Marsset, M., DeMeo, F.E., Bus, S.J., Geem, J., Ishiguro, M., Im, M., Kuroda, D., Vernazza, P., 2021. Discovery of two TNO-like bodies in the asteroid belt. *ApJL* 916, L6. <https://doi.org/10.3847/2041-8213/ac0f05>.
- Hilton, C.D., Ash, R.D., Walker, R.J., 2022. Chemical characteristics of iron meteorite parent bodies. *Geochim. Cosmochim. Acta* 318, 112–125. <https://doi.org/10.1016/j.gca.2021.11.035>.
- Horan, M.F., Walker, R.J., Morgan, J.W., Grossman, J.N., Rubin, A.E., 2003. Highly siderophile elements in chondrites. *Chem. Geol.* 196, 27–42. [https://doi.org/10.1016/S0009-2541\(02\)00405-9](https://doi.org/10.1016/S0009-2541(02)00405-9).
- Horan, M.F., Alexander, C.M.O., Walker, R.J., 2009. Highly siderophile element evidence for early solar system processes in components from ordinary chondrites. *Geochim. Cosmochim. Acta* 73, 6984–6997. <https://doi.org/10.1016/j.gca.2009.08.022>.
- Howard, K.T., Alexander, C.M.O., Schrader, D.L., Dyl, K.A., 2015. Classification of hydrous meteorites (CR, CM and C2 ungrouped) by phyllosilicate fraction: PSD-XRD modal mineralogy and planetesimal environments. *Geochim. Cosmochim. Acta* 149, 206–222. <https://doi.org/10.1016/j.gca.2014.10.025>.
- Jarosewich, E., 1990. Chemical analyses of meteorites: a compilation of stony and iron meteorite analyses. *Meteoritics* 25, 323–337. <https://doi.org/10.1111/j.1945-5100.1990.tb00717.x>.
- Jarosewich, E., 2006. Chemical analyses of meteorites at the Smithsonian Institution: an update. *Meteoritics Planet. Sci.* 41, 1381–1382. <https://doi.org/10.1111/j.1945-5100.2006.tb00528.x>.
- Jedicke, R., Sercel, J., Gillis-Davis, J., Morenz, K.J., Gertsch, L., 2018. Availability and delta-v requirements for delivering water extracted from near-Earth objects to cis-lunar space. *Planet. Space Sci.* 159, 28–42. <https://doi.org/10.1016/j.pss.2018.04.005>.
- Jehle, A., Scott, E., Centers, R., 2020. A planetary sunshade built from space resources. In: *ASCEND 2020*. Presented at the ASCEND 2020. American Institute of Aeronautics and Astronautics, Virtual Event. <https://doi.org/10.2514/6.2020-4077>.
- Johnson, C.A., Prinz, M., 1993. Carbonate compositions in CM and CI chondrites and implications for aqueous alteration. *Geochim. Cosmochim. Acta* 57, 2843–2852. [https://doi.org/10.1016/0016-7037\(93\)90393-B](https://doi.org/10.1016/0016-7037(93)90393-B).
- Kargel, J.S., 1994. Metalliferous asteroids as potential sources of precious metals. *J. Geophys. Res.* 99, 21129. <https://doi.org/10.1029/94JE02141>.
- Koblitz, J., 2003. *MetBase-Meteorite Data Retrieval Software*, vol. 6. MetBase version.
- Kornacki, A.S., Wood, J.A., 1985. Mineral chemistry and origin of spinel-rich inclusions in the Allende CV3 chondrite. *Geochim. Cosmochim. Acta* 49, 1219–1237. [https://doi.org/10.1016/0016-7037\(85\)90012-2](https://doi.org/10.1016/0016-7037(85)90012-2).
- Kurokawa, H., Shibuya, T., Sekine, Y., Ehlmann, B.L., Usui, F., Kikuchi, S., Yoda, M., 2022. Distant Formation and differentiation of outer main belt asteroids and carbonaceous chondrite parent bodies. *AGU Advances* 3. <https://doi.org/10.1029/2021AV000568>.
- Lewis, J.S., 1996. *Mining the Sky: Untold Riches from the Asteroids, Comets, and Planets*. Reading.
- Lodders, K., 2003. Solar system abundances and condensation temperatures of the elements. *APJ (Acta Pathol. Jpn.)* 591, 1220–1247. <https://doi.org/10.1086/375492>.

- Ma, M.-S., Schmitt, R.A., 1979. Genesis of the cumulate eucrites Serra de Magé and moore county: a geochemical study. *Meteoritics* 14, 81–89. <https://doi.org/10.1111/j.1945-5100.1979.tb00481.x>.
- Mahlke, M., Carry, B., Mattei, P.-A., 2022. Asteroid Taxonomy from Cluster Analysis of Spectrometry and Albedo arXiv:2203.11229.
- Mason, B., Jarosewich, E., 1973. The barea, dyarrl island, and emery meteorites, and a review of the mesosiderites. *Mineral. Mag.* 39 (302), 204–215. <https://doi.org/10.1017/minmag.1973.039.302.08>.
- McCoy, T.J., Ehlmann, A.J., Benedix, G.K., Keil, K., Wasson, J.T., 1996. The Lueders, Texas, IAB iron meteorite with silicate inclusions. *Meteoritics Planet Sci.* 31, 419–422. <https://doi.org/10.1111/j.1945-5100.1996.tb02081.x>.
- McCoy, T.J., Walker, R.J., Goldstein, J.I., Yang, J., McDonough, W.F., Rumble, D., Chabot, N.L., Ash, R.D., Corrigan, C.M., Michael, J.R., Kotula, P.G., 2011. Group IVA irons: new constraints on the crystallization and cooling history of an asteroidal core with a complex history. *Geochem. Cosmochim. Acta* 75, 6821–6843. <https://doi.org/10.1016/j.gca.2011.09.006>.
- Metzger, P.T., Muscatello, A., Mueller, R.P., Mantovani, J., 2013. Affordable, rapid bootstrapping of the space industry and solar system civilization. *J. Aero. Eng.* 26, 18–29. [https://doi.org/10.1061/\(ASCE\)AS.1943-5525.0000236](https://doi.org/10.1061/(ASCE)AS.1943-5525.0000236).
- Nakamura, T., Noguchi, T., Tanaka, M., Zolensky, M.E., Kimura, M., Tsuchiyama, A., Nakato, A., Ogami, T., Ishida, H., Uesugi, M., Yada, T., Shirai, K., Fujimura, A., Okazaki, R., Sandford, S.A., Ishibashi, Y., Abe, M., Okada, T., Ueno, M., Mukai, T., Yoshikawa, M., Kawaguchi, J., 2011. Itokawa dust particles: a direct link between S-type asteroids and ordinary chondrites. *Science* 333, 1113–1116. <https://doi.org/10.1126/science.1207758>.
- Northey, S., Mohr, S., Mudd, G.M., Weng, Z., Giurco, D., 2014. Modelling future copper ore grade decline based on a detailed assessment of copper resources and mining. *Resour. Conserv. Recycl.* 83, 190–201. <https://doi.org/10.1016/j.resconrec.2013.10.005>.
- Okabayashi, S., Yokoyama, T., Nakanishi, N., Iwamori, H., 2019. Fractionation of highly siderophile elements in metal grains from unequilibrated ordinary chondrites: implications for the origin of chondritic metals. *Geochem. Cosmochim. Acta* 244, 197–215. <https://doi.org/10.1016/j.gca.2018.10.003>.
- Palme, H., Lodders, K., Jones, A., 2014. Solar system abundances of the elements. In: *Treatise on Geochemistry*. Elsevier, pp. 15–36. <https://doi.org/10.1016/B978-0-08-095975-7.00118-2>.
- Petaev, M.I., Jacobsen, S.B., 2004. Differentiation of metal-rich meteoritic parent bodies: I. Measurements of PGEs, Re, Mo, W, and Au in meteoritic Fe-Ni metal. *Meteoritics Planet Sci.* 39, 1685–1697. <https://doi.org/10.1111/j.1945-5100.2004.tb00066.x>.
- Rivkin, A.S., DeMeo, F.E., 2019. How many hydrated NEOs are there? *JGR Planets* 124, 128–142. <https://doi.org/10.1029/2018JE005584>.
- Rubin, A.E., 2018. Carbonaceous and noncarbonaceous iron meteorites: differences in chemical, physical, and collective properties. *Meteoritics Planet Sci.* 53, 2357–2371. <https://doi.org/10.1111/maps.13128>.
- Sánchez, P., Scheeres, D.J., 2014. The strength of regolith and rubble pile asteroids. *Meteorit. Planet. Sci.* 49, 788–811. <https://doi.org/10.1111/maps.12293>.
- Sanchez, J.A., Reddy, V., Kelley, M.S., Cloutis, E.A., Bottke, W.F., Nesvorný, D., Lucas, M.P., Hardersen, P.S., Gaffey, M.J., Abell, P.A., Corre, L.L., 2014. Olivine-dominated asteroids: mineralogy and origin. *Icarus* 228, 288–300. <https://doi.org/10.1016/j.icarus.2013.10.006>.
- Shearer, C.K., Burger, P.V., Papike, J.J., Sharp, Z.D., McKEEGAN, K.D., 2011. Fluids on differentiated asteroids: evidence from phosphates in differentiated meteorites GRA 06128 and GRA 06129: fluids on differentiated asteroids. *Meteoritics Planet Sci.* 46, 1345–1362. <https://doi.org/10.1111/j.1945-5100.2011.01233.x>.
- Shepard, M.K., Clark, B.E., Nolan, M.C., Howell, E.S., Magri, C., Giorgini, J.D., Benner, L.A.M., Ostro, S.J., Harris, A.W., Warner, B., Pray, D., Pravec, P., Fauerbach, M., Bennett, T., Klotz, A., Behrend, R., Correia, H., Coloma, J., Casulli, S., Rivkin, A., 2008. A radar survey of M- and X-class asteroids. *Icarus* 195, 184–205. <https://doi.org/10.1016/j.icarus.2007.11.032>.
- Shepard, M.K., Clark, B.E., Ockert-Bell, M., Nolan, M.C., Howell, E.S., Magri, C., Giorgini, J.D., Benner, L.A.M., Ostro, S.J., Harris, A.W., Warner, B.D., Stephens, R.D., Mueller, M., 2010. A radar survey of M- and X-class asteroids II. Summary and synthesis. *Icarus* 208, 221–237. <https://doi.org/10.1016/j.icarus.2010.01.017>.
- Shepard, M.K., Taylor, P.A., Nolan, M.C., Howell, E.S., Springmann, A., Giorgini, J.D., Warner, B.D., Harris, A.W., Stephens, R., Merline, W.J., Rivkin, A., Benner, L.A.M., Coley, D., Clark, B.E., Ockert-Bell, M., Magri, C., 2015. A radar survey of M- and X-class asteroids. III. Insights into their composition, hydration state, & structure. *Icarus* 245, 38–55. <https://doi.org/10.1016/j.icarus.2014.09.016>.
- Sowers, G.F., 2021. The business case for lunar ice mining. *New Space* 9, 77–94. <https://doi.org/10.1089/space.2020.0045>.
- Srinivasan, P., Dunlap, D.R., Agee, C.B., Wadhwa, M., Coleff, D., Ziegler, K., Zeigler, R., McCubbin, F.M., 2018. Silica-rich volcanism in the early solar system dated at 4.565 Ga. *Nat. Commun.* 9, 3036. <https://doi.org/10.1038/s41467-018-05501-0>.
- Sunshine, J.M., Connolly, H.C., McCoy, T.J., Bus, S.J., La Croix, L.M., 2008. Ancient asteroids enriched in refractory inclusions. *Science* 320, 514–517. <https://doi.org/10.1126/science.1154340>.
- Swindle, T.D., Kring, D.A., Burkland, M.K., Hill, D.H., Boynton, W.V., 1998. Noble gases, bulk chemistry, and petrography of olivine-rich achondrites Eagles Nest and Lewis Cliff 88763: comparison to brachinites. *Meteoritics Planet Sci.* 33, 31–48. <https://doi.org/10.1111/j.1945-5100.1998.tb01605.x>.
- Tholen, D.J., 1984. Asteroid Taxonomy from Cluster Analysis of Photometry (Ph.D. Thesis).
- Tornabene, H.A., 2020. Insights to the Genetics, Age and Crystallization of Group IC and LIC Iron Meteorites. University of Maryland, College Park.
- Tornabene, H.A., Hilton, C.D., Birmingham, K.R., Ash, R.D., Walker, R.J., 2020. Genetics, age and crystallization history of group IIC iron meteorites. *Geochem. Cosmochim. Acta* 288, 36–50. <https://doi.org/10.1016/j.gca.2020.07.036>.
- U.S. Geological Survey, 2022. Mineral Commodity Summaries 2022. U.S. Geological Survey, p. 202. <https://doi.org/10.3133/mcs2022>.
- Usui, T., McSween, H.Y., 2007. Geochemistry of 4 Vesta based on HED meteorites: prospective study for interpretation of gamma ray and neutron spectra for the Dawn mission. *Meteoritics Planet Sci.* 42, 255–269. <https://doi.org/10.1111/j.1945-5100.2007.tb00231.x>.
- van der Zee, L.F., Pelzer, R., Marais, J.H., 2013. The combined cost effect of carbon tax, ECS and MYPD3 tariffs on the gold mining industry of South Africa. In: 2013 Proceedings of the 10th Industrial and Commercial Use of Energy Conference. Cape Peninsula University of Technology, pp. 1–8, 1–8.
- van Kooten, E.M.M.E., Kubik, E., Siebert, J., Heredia, B.D., Thomsen, T.B., Moynier, F., 2022. Metal compositions of carbonaceous chondrites. *Geochem. Cosmochim. Acta* 321, 52–77. <https://doi.org/10.1016/j.gca.2022.01.008>.
- Viikinkoski, M., Vernazza, P., Hanuš, J., Le Coroller, H., Tazhenova, K., Carry, B., Marsset, M., Drouard, A., Marchis, F., Fetick, R., Fusco, T., Durech, J., Birlan, M., Berthier, J., Bartzak, P., Dumas, C., Castillo-Rogez, J., Cipriani, F., Colas, F., Ferrais, M., Grice, J., Jehin, E., Jorda, L., Kaasalainen, M., Kryszczyńska, A., Lamy, P., Marciniak, A., Michalowski, T., Michel, P., Pajuelo, M., Podlowska-Gaca, E., Santana-Ros, T., Tanga, P., Vachier, F., Vigan, A., Warner, B., Witaske, O., Yang, B., 2018. (16) Psyche: a mesosiderite-like asteroid? *A&A* 619, L3. <https://doi.org/10.1051/0004-6361/201834091>.
- Walker, R.J., McDonough, W.F., Honesto, J., Chabot, N.L., McCoy, T.J., Ash, R.D., Bellucci, J.J., 2008. Modeling fractional crystallization of group IVB iron meteorites. *Geochem. Cosmochim. Acta* 72, 2198–2216. <https://doi.org/10.1016/j.gca.2008.01.021>.
- Wasson, J.T., 2017. Formation of non-magmatic iron-meteorite group IIE. *Geochem. Cosmochim. Acta* 197, 396–416. <https://doi.org/10.1016/j.gca.2016.09.043>.
- Wasson, J.T., Huber, H., 2006. Compositional trends among IID irons; their possible formation from the P-rich lower magma in a two-layer core. *Geochem. Cosmochim. Acta* 70, 6153–6167. <https://doi.org/10.1016/j.gca.2006.01.032>.
- Wasson, J.T., Huber, H., Malvin, D.J., 2007. Formation of IIAB iron meteorites. *Geochem. Cosmochim. Acta* 71, 760–781. <https://doi.org/10.1016/j.gca.2006.09.032>.
- Wasson, J.T., Richardson, J.W., 2001. Fractionation trends among IVA iron meteorites: contrasts with IIAB trends. *Geochem. Cosmochim. Acta* 65, 951–970. [https://doi.org/10.1016/S0016-7037\(00\)00597-4](https://doi.org/10.1016/S0016-7037(00)00597-4).
- Weisberg, M.K., Kimura, M., 2012. The unequilibrated enstatite chondrites. *Geochemistry* 72, 101–115. <https://doi.org/10.1016/j.chemer.2012.04.003>.
- Weyrauch, M., Zipfel, J., Weyer, S., 2021. The relationship of CH, CB, and CR chondrites: constraints from trace elements and Fe-Ni isotope systematics in metal. *Geochem. Cosmochim. Acta* 308, 291–309. <https://doi.org/10.1016/j.gca.2021.06.009>.
- Worsham, E.A., Birmingham, K.R., Walker, R.J., 2016. Siderophile element systematics of IAB complex iron meteorites: new insights into the formation of an enigmatic group. *Geochem. Cosmochim. Acta* 188, 261–283. <https://doi.org/10.1016/j.gca.2016.05.019>.
- Zhang, B., Chabot, N.L., Rubin, A.E., Humayun, M., Boesenberg, J.S., van Niekirk, D., 2022a. Chemical study of group IIIF iron meteorites and the potentially related pallasites Zinder and Northwest Africa 1911. *Geochem. Cosmochim. Acta* 323, 202–219. <https://doi.org/10.1016/j.gca.2022.02.004>.
- Zhang, B., Chabot, N.L., Rubin, A.E., 2022b. Compositions of carbonaceous-type asteroidal cores in the early solar system. *Sci. Adv.* 8, eabo5781. <https://doi.org/10.1126/sciadv.abo5781>.